



Brief communication

Experimental study on effect of relative humidity on heat transfer of an evaporating water droplet in air flow

Akitoshi Fujita, Ryoichi Kurose*, Satoru Komori

Department of Mechanical Engineering and Science, and Advanced Research Institute of Fluid Science and Engineering, Kyoto University, Yoshida-honmachi, Kyoto-shi, Kyoto 606-8501, Japan

ARTICLE INFO

Article history:

Received 25 May 2009

Received in revised form 27 October 2009

Accepted 30 October 2009

Available online 5 November 2009

Keywords:

Heat transfer

Evaporation

Droplet

Humidity

ABSTRACT

Dispersed water droplets are often seen in environmental air flows in rain, cloud, mist, sea spray and so on. It is therefore of great importance to precisely estimate heat transfer between water droplets and atmospheric air in developing a reliable climate model. The purpose of this study is to fabricate the measurement system for the temperature of a small water droplet in air flow under the controlled relative humidity condition and to investigate the effect of relative humidity on heat transfer across the surface of an evaporating water droplet in air flow. The results show that the droplet temperature decreases in the low-relative-humidity condition, whereas it increases in the high-relative-humidity condition. Nusselt number on the droplet surface is not affected by the relative humidity.

© 2009 Elsevier Ltd. All rights reserved.

1. Introduction

Dispersed water droplets are often seen in environmental air flows in rain, cloud, mist, sea spray and so on. It is therefore of great importance to precisely estimate heat transfer between water droplets and atmospheric air in developing a reliable climate model. Very recently, Kurose et al. (2009) investigated the heat transfer across the surface of an evaporating water droplet in air flow by applying a direct numerical simulation (DNS) to flows both inside and outside the droplet. They found that the droplet temperature decreases in the low-relative-humidity condition, whereas it increases in the high-relative-humidity condition and suggested that this difference is caused by the heat balance of evaporative heat loss and convective heat gain from ambient air at the droplet surface. However, this behavior has not been experimentally observed yet. Although there exist some experiments in which evaporation rate and/or heat transfer rate of a water droplet in air flow are estimated (e.g., Beard and Pruppacher, 1971; Richards and Richards, 1998), effect of the relative humidity has never been paid attention to. The purpose of this study is therefore to fabricate the measurement system for the temperature of a small water droplet in air flow under the controlled relative humidity condition and to experimentally verify the DNS results.

2. Experiments

Fig. 1 shows the schematic of experimental apparatus. The air provided by a blower or a dry air canister is supplied to a test section of a vertical wind tunnel through a constant temperature tank, a buffer and a rectification section. The air relative humidity, temperature and flow rate are controlled by adjusting the state of wet filter set in the blower, the temperature in the constant temperature tank, and the fan rotating speed set at the inlet of wind tunnel. The air flow rate from the blower or dry air canister is controlled to keep an atmospheric pressure in the buffer by monitoring the precision micro differential manometer (SIBATA ISP-35S).

Fig. 2 shows the details of the test section and measurement system. The test section of the vertical wind tunnel consisted of a 0.2 m long square pipe with a cross-section of 0.05 m × 0.05 m, which is made of polymethylmethacrylate (PMMA). The mean flow velocity, temperature and relative humidity in the test section are measured by a particle image velocimetry (PIV) (DANTEC DYNAMICS DC-PIV System), a thermocouple (ANRITSU TM-5898) and a digital hygrometer (B&K PRECISION 725), respectively. The mean particle diameter of the tracer particle generated by a fog generator (DANTEC DYNAMICS SAFEX Fog Generator FOG 2004) for the PIV is approximately 1.0 μm. A single droplet produced using a syringe pump (HARVARD PHD2000) is suspended at the tip of needle (diameter = 0.08 mm) in the test section. Water for the droplet is distilled water. The surface temperature and diameter of a droplet are simultaneously measured by an infrared thermography (NIPPON AVIONICS TVS-8502) and a digital camera (NIKON D1x), respectively. These image sizes and resolutions are 256 × 236

* Corresponding author. Tel./fax: +81 75 753 9218.

E-mail address: kurose@mech.kyoto-u.ac.jp (R. Kurose).

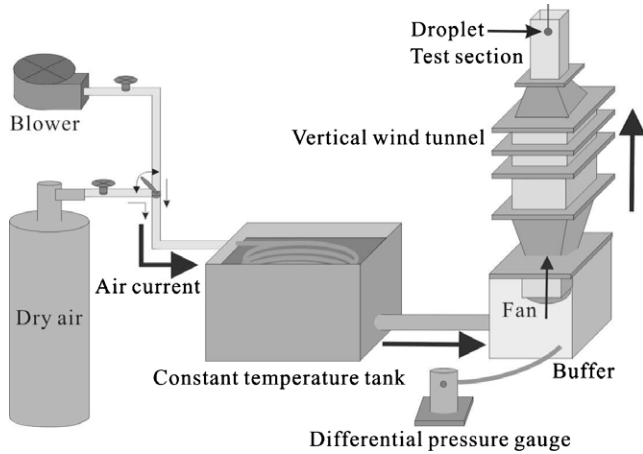


Fig. 1. Schematic of experimental apparatus.

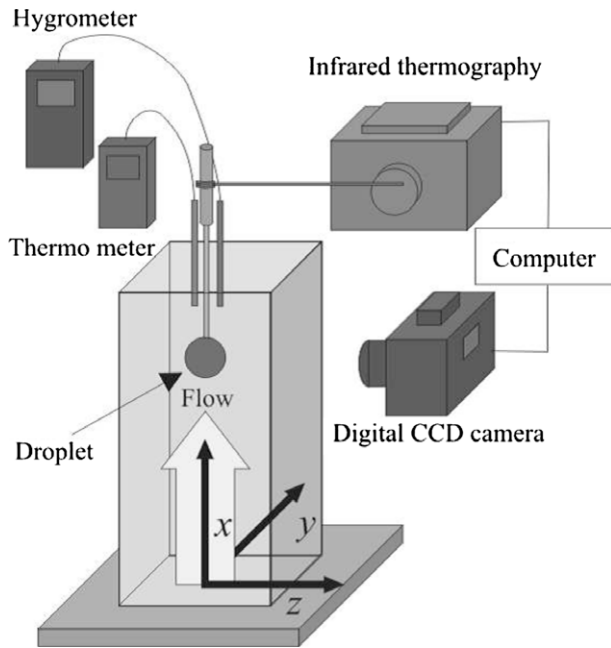


Fig. 2. Schematic of test section and measurement system.

pixels, 0.3 mm and 3008×1960 pixels, $4 \mu\text{m}$, respectively. For the use of the infrared thermography, a quartz glass through which the radiation can pass was installed in a part of the wall of the test section where the droplet is located. In this condition, it is inferred that the infrared energy only from thin film of $10 \mu\text{m}$ depth of the droplet surface is measured by the infrared thermography (e.g., Modest, 2003).

In Fig. 3, The typical horizontal (z) distributions of the mean streamwise (x) velocity \bar{U} , root mean squared values (rms) of the streamwise velocity fluctuations u' , mean air temperature \bar{T}_{air} , and mean relative humidity \bar{Hu} at the streamwise location of $x = 100$ mm from the bottom of the test section, where the droplet is placed, are shown. The uniform flow field with negligibly weak velocity fluctuation is observed to be attained in the central region of the test section. In this case, the uniform air velocity U_c is 0.8 m/s, the uniform air temperature $T_{air,c}$ is 303.15 K and the uniform relative humidity Hu_c is 30%. It was also confirmed that the similar trends are obtained in the different uniform flow velocity and relative humidity cases.

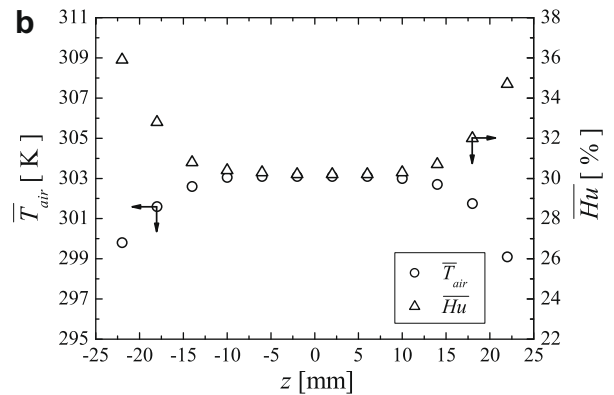
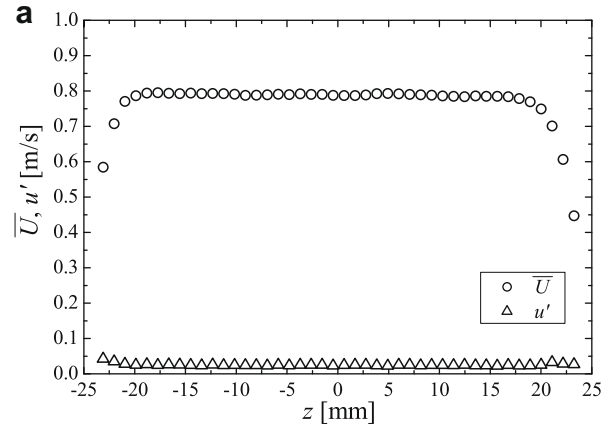


Fig. 3. Horizontal distributions of mean and rms streamwise velocity, \bar{U} and u' , mean air temperature \bar{T}_{air} and mean relative humidity \bar{Hu} : (a) \bar{U} and u' ; (b) \bar{T}_{air} and \bar{Hu} .

Fig. 4 shows the typical thermography image of the droplet surface temperature $T_{s,N}$ and its quantitative distribution on the line A–A' at a certain moment. In Fig. 4b, N shows the number of the measurement position. It is found that although the thermography image is relatively coarse (as described below, the droplet diameter is 1.2 mm so that the resolution is about 0.3 mm), the temperature exhibits uniform value in the central region. Hence, this uniform temperature is regarded as the droplet surface temperature T_s in this study.

The experiment was conducted under the conditions that the initial droplet diameter d_0 was 1.2 mm, the initial droplet surface temperature $T_{s,0}$ was 288.15 K, and the air temperature in the central region of the test section $T_{air,c}$ was 303.15 K. The uniform air velocity U_c and relative humidity Hu_c were varied as $U_c = 0.4, 0.8, 1.6$ and 2.0 m/s and $Hu_c = 0$ and 30%, respectively. The absolute error of $T_{air,c}$ was 0.3 K, and those of Hu_c were 2% for $Hu_c = 0\%$ and 0.2% for $Hu_c = 30\%$, respectively. The droplet Reynolds numbers Re_d defined as $Re_d = \rho_g U_c d_0 / \mu_g$ were about 30, 60, 120 and 150, respectively. Here, ρ_g , d_0 and μ_g are the density ($=1.15 \text{ kg/m}^3$), the initial droplet diameter and the viscosity ($=1.87 \times 10^{-5} \text{ Pa s}$) of the air, respectively. These values are based on air temperature at 303.15 K. These conditions were similar to those of the DNS in Kurose et al. (2009). The droplet diameter and surface temperature were recorded for 30 s.

3. Results and discussion

Fig. 5 shows the effects of relative humidity Hu_c and droplet Reynolds number Re_d on the time variations of the droplet diame-

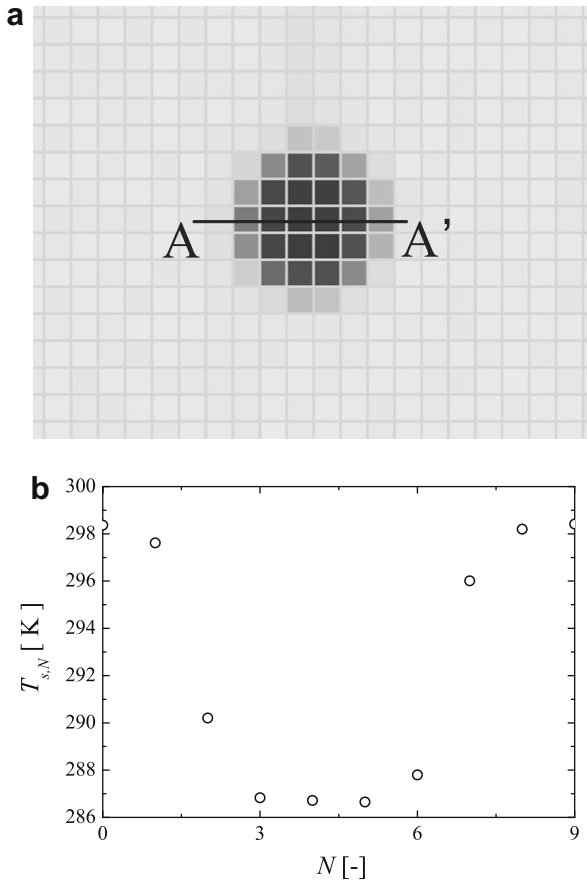


Fig. 4. Droplet surface temperature $T_{s,N}$: (a) thermography image; (b) distribution on the line A–A’.

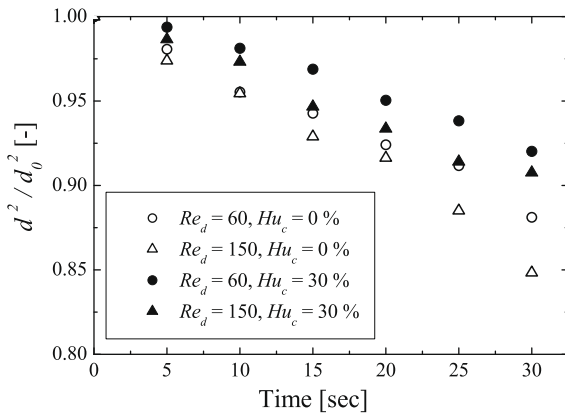


Fig. 5. Time variations of droplet diameter d^2/d_0^2 .

ter d based on d_0 , d^2/d_0^2 . It is found that d^2/d_0^2 monotonously decreases with time in all cases and that the reduction rate becomes larger as Hu_c decreases or Re_d increases.

The time variation of the droplet surface temperature, $T_s - T_{s,0}$, is shown in Fig. 6. The droplet surface temperature increases in the high-relative-humidity condition of $Hu_c = 30\%$, whereas it decreases in the low-relative-humidity condition of $Hu_c = 0\%$ in spite of the fact that the initial droplet temperature is lower than the air temperature. This is because for $Hu_c = 0\%$ the evaporation is facilitated by the low relative humidity, which increases the evaporative heat loss compared to the heat gain from the higher-temperature ambient air. These tendencies well agree with and

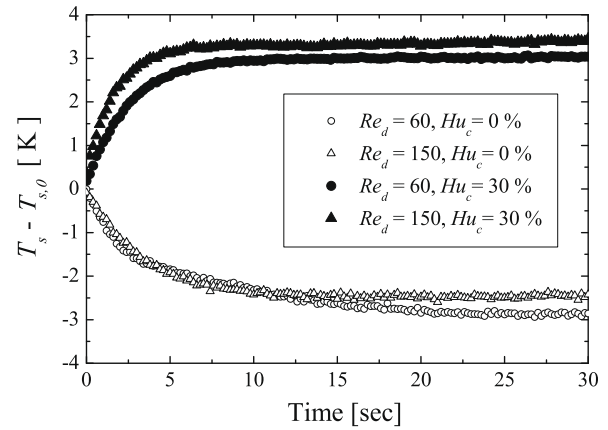


Fig. 6. Time variations of droplet surface temperature, $T_s - T_{s,0}$.

therefore support the DNS results by Kurose et al. (2009). It is also found that in all cases, the droplet surface temperature approaches constant values. This is because the evaporative heat loss from the droplet equilibrates with the heat gain from the ambient air under the given temperature condition. Since the convective heat transfer is generally enhanced for higher Re_d , the convergence temperature tends to be higher in the higher Re_d case.

To further make sure of the correspondence in the droplet temperature variation between the present experiment and the DNS by Kurose et al. (2009), the DNS was performed in the same conditions as the experiment and their results are compared in Fig. 7. Although the numerical methods and procedure are essentially the same as Kurose and Komori (1999), Sugioka and Komori (2007) and Kurose et al. (2009), the decrease in the droplet Reynolds numbers Re_d due to the evaporation is newly taken into account here. It is found that for both the experiment and DNS, the droplet temperature increases in the high-relative-humidity condition, whereas it decreases in the low-relative-humidity condition. The quantitative discrepancy between the experiment and DNS for the low-relative-humidity condition is considered due to time variation of the relative humidity from the initial value (probably 60–80%) to the steady value (i.e., 0%). This shows the difficulty to control the initial relative humidity and the limitation of our experiment.

Fig. 8 shows the relationship between Nusselt number Nu and droplet Reynolds number Re_d , together with the previous experimental data by Beard and Pruppacher (1971) and Cliff et al.

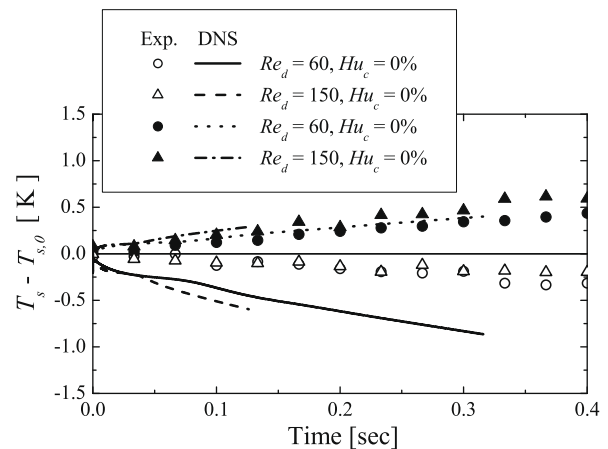


Fig. 7. Comparison of time variation of droplet surface temperature, $T_s - T_{s,0}$, between experiment and DNS.

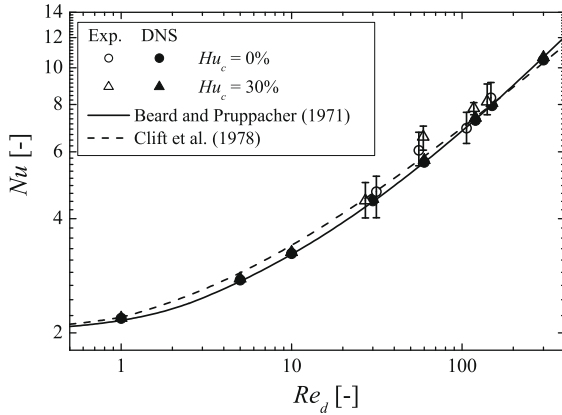


Fig. 8. Relationship between Nusselt number Nu and droplet Reynolds number Re_d .

(1978) in which the effect of the relative humidity is neglected. In addition, although the Nusselt number tends to decay with time (e.g., Sirignano, 1993), the values only for the steady state of $t = 30$ s are calculated here, as follows: Nu is defined by

$$Nu = \frac{hd}{\lambda_g}, \quad (1)$$

where λ_g is the thermal conductivity of the air ($=2.64 \times 10^{-2}$ J/(s m K)) for the air temperature at 303.15 K. h is the heat transfer coefficient. The derivation procedure of h is shown below. The heat transfer rate to a droplet Q_G is described as

$$Q_G = A_d h (T_g - T_s), \quad (2)$$

where A_d is the surface area of a droplet. Q_G is also given by the contributions of the evaporative heat loss Q_E , droplet temperature change Q_S and radiation Q_R as

$$Q_G = Q_E + Q_S - Q_R, \quad (3)$$

$$Q_E = A_d L_v \dot{m}, \quad (4)$$

$$Q_S = \rho_w V_d C_{p,w} \frac{dT_s}{dt}, \quad (5)$$

$$Q_R = \epsilon \sigma A_d (T_{wall}^4 - T_s^4). \quad (6)$$

Here, L_v , ρ_w and $C_{p,w}$ are the latent heat ($=2.46 \times 10^6$ J/kg), the density ($=9.99 \times 10^2$ kg/m³) and the specific heat capacity ($=4.19 \times 10^3$ J/(kg K)) of the droplet, respectively. These values are based on water temperature at 288.15 K. \dot{m} , V_d and T_{wall} are the droplet evaporation rate per unit area per unit time, the volume of the droplet and the wall temperature of the test section, respectively. ϵ and σ are the emissivity ($=0.95$) and the Stefan–Boltzmann constant ($=5.67 \times 10^{-8}$ J/(s m² K⁴)). The amount of evaporation mass per unit time from the

droplet $A_d \dot{m}$ in Eq. (4) is estimated using the profile in Fig. 5. In Eq. (5), the value of dT_s/dt is the value at $t = 30$ s. Eq. (5) is obtained under the assumption that the time variation rate of the average droplet temperature becomes almost equal to that of the average droplet surface temperature dT_s/dt in a short time less than 0.3 s. The validity of this assumption was verified by DNS. In the case of $Re_d = 150$, for example, the average values of Q_E , Q_S and Q_R [J/s] are 1.44×10^{-2} , -3.79×10^{-6} , 3.98×10^{-4} for $Hu_c = 0\%$ and 8.86×10^{-3} , 6.90×10^{-6} , 1.26×10^{-4} for $Hu_c = 30\%$, respectively. It is found that the present Nu is in good agreement with the previous experimental data by Beard and Pruppacher (1971) and Clift et al. (1978) that Nu is hardly affected by the relative humidity.

4. Conclusions

Effect of relative humidity on heat transfer across the surface of an evaporating water droplet in air flow was experimentally investigated. The results showed that the droplet temperature decreases in the low-relative-humidity condition, whereas it increases in the high-relative-humidity condition, which agree well with the DNS results by Kurose et al. (2009). It was also found that the Nusselt number on the droplet surface is not affected by the relative humidity.

Acknowledgments

The authors would like to thank T. Morishita for his help in conducting experiments. This work was supported by Grant-in-Aid for Scientific Research (Nos. 19206023 and 20686015) and partially supported by Core Research for Evolutional Science and Technology (CREST) Program “Advanced Model Development and Simulations for Disaster Countermeasures” of Japan Science and Technology Agency (JST).

References

- Beard, K.V., Pruppacher, H.R., 1971. A wind tunnel investigation of the rate of evaporation of small water drops falling at terminal velocity in air. *J. Atmos. Sci.* 28, 1455–1464.
- Clift, R., Grace, J.R., Weber, M.E., 1978. *Bubbles, Drops, and Particles*. Academic Press, New York.
- Kurose, R., Komori, S., 1999. Drag and lift forces on a rotating sphere in a linear shear flow. *J. Fluid Mech.* 384, 183–206.
- Kurose, R., Fujita, A., Komori, S., 2009. Effect of relative humidity on heat transfer across the surface of an evaporating water droplet in air flow. *J. Fluid Mech.* 624, 57–67.
- Modest, M.F., 2003. *Radiative Heat Transfer*, second ed. Academic Press, New York.
- Richards, C.D., Richards, R.F., 1998. Transient temperature measurements in a convectively cooled droplet. *Exp. Fluids* 25, 392–400.
- Sirignano, W.A., 1993. *Fluid dynamics of sprays* – 1992 Freeman scholar lecture. *J. Fluids Eng.* 115, 345–378.
- Sugioka, K., Komori, S., 2007. Drag and lift forces acting on a spherical water droplet in homogeneous linear shear air flow. *J. Fluid Mech.* 570, 155–175.